Journal of Atmospheric and Terrestrial Physics, Vol. 52, No. 6–8, pp. 501–517, 1990.
Printed in Great Britain.

0021–9169/90 $3.00 + .00
Pergamon Press plc

Measuring ion temperatures and studying the ion energy balance in the high-latitude ionosphere

K. J. WINSER,† M. LOCKWOOD,† G. O. L. JONES,‡ H. RISHBETH§ and M. G. ASHFORD§

† Rutherford Appleton Laboratory, Chilton, Didcot OX11 0QX, U.K.; ‡ Physics Department, University College of Wales, Aberystwyth SY23 3BZ, U.K.; § Physics Department, University of Southampton, Southampton SO9 5NH, U.K.

(*Received in final form* 17 *April* 1990)

Abstract—Data are presented for a nighttime ion heating event observed by the EISCAT radar on 16 December 1988. In the experiment, the aspect angle between the radar beam and the geomagnetic field was fixed at 54.7°, which avoids any ambiguity in derived ion temperature caused by anisotropy in the ion velocity distribution function. The data were analyzed with an algorithm which takes account of the non-Maxwellian line-of-sight ion velocity distribution. During the heating event, the derived spectral distortion parameter (D^*) indicated that the distribution function was highly distorted from a Maxwellian form when the ion drift increased to 4 km s^{-1}.

The true three-dimensional ion temperature was used in the simplified ion balance equation to compute the ion mass during the heating event. The ion composition was found to change from predominantly O^+ to mainly molecular ions. A theoretical analysis of the ion composition, using the MSIS86 model and published values of the chemical rate coefficients, accounts for the order-of-magnitude increase in the atomic/molecular ion ratio during the event, but does not successfully explain the very high proportion of molecular ions that was observed.

1. INTRODUCTION

In the presence of large d.c. electric fields, the ion velocity distribution function in the high-latitude, *F*-region ionosphere becomes anisotropic and significantly distorted from the Maxwellian form associated with thermal equilibrium (ST-MAURICE and SCHUNK, 1979). Such distortions from thermal equilibrium give rise to characteristic spectra of signals received by an incoherent scatter radar (see, for example, RAMAN *et al.*, 1981; HUBERT, 1984). The spectral shape is determined by the line-of-sight ion velocity distribution and, by assuming a suitable form for this, it is possible to derive a line-of-sight ion temperature from the radar measurements. LOCKWOOD and WINSER (1988) have presented rigorous definitions of ion temperature and have clearly distinguished between the line-of-sight and three-dimensional ion temperature, and pointed out that only the latter can be used in energy considerations.

Recent ground-based radar measurements have provided confirmation that the ion velocity distribution can become anisotropic when the electric fields are large (PERRAUT *et al.*, 1984; LØVHAUG and FLÅ, 1986). Clear evidence for the presence of highly non-Maxwellian distributions has also been presented by LOCKWOOD *et al.* (1987), WINSER *et al.* (1987), MOORCROFT and SCHLEGEL (1988), WINSER *et al.* (1989), SUVANTO *et al.* (1989) and LOCKWOOD *et al.* (1989). The first experimental evidence that the observed incoherent scatter spectra under such conditions were sensitive to aspect angle, as predicted theoretically, was presented by WINSER *et al.* (1987, 1989), and these along with other workers (MOORCROFT and SCHLEGEL, 1988; SUVANTO, 1988; SUVANTO *et al.*, 1989) have shown that ionospheric parameters derived from such data with the assumption of a Maxwellian velocity distribution are in serious error.

In analyzing incoherent scatter spectra measured during conditions of large electric field, there are two problems to be considered: first, the ion temperature exhibits a strong anisotropy which must be accounted for if energy balance arguments are to be used; and second, the distribution of line-of-sight ion velocities departs from a Maxwellian form (at least for look directions away from 0° aspect angle), and any interpretation of the data using the standard assumption of a Maxwellian distribution leads to errors in the derived ionospheric parameters.

2. EXPERIMENTAL PROCEDURE

To remove the first of the difficulties described above, we devised the ISOA experiment, in which the angle, ψ, between the direction of the Tromsø radar beam and the geomagnetic field (referred to as the aspect angle) remained fixed at 54.7° [= arc sin $\sqrt{(2/3)}$]. The Tromsø antenna azimuth and elevation were 360.0 and 44.8°, respectively. From the definition of one-dimensional temperature, it can be shown that the line-of-sight (l-o-s) ion temperature, T_f, (for an ion velocity distribution function which is symmetric in the field-parallel direction) is given by:

$$T_f = T_\parallel \cos^2 \psi + T_\perp \sin^2 \psi \quad (1)$$

and at $\psi = 54.7°$ this is the same as the 'real' (kinetic) three-dimensional temperature which, for a gyrotropic distribution function, is defined as (LOCKWOOD and WINSER, 1988):

$$T_i = (T_\parallel + 2T_\perp)/3. \quad (2)$$

The parallel and perpendicular ion temperatures, $T_\parallel$ and $T_\perp$, are defined in the same way as T_f for aspect angles, ψ, of 0 and 90°, respectively. Both equations (1) and (2) arise from the definition of ion temperature and are valid for any form of the distribution function which is gyrotropic and symmetric with respect to the magnetic field direction. As both these conditions are predicted to be met in the F-region (ST-MAURICE and SCHUNK, 1979; KIKUCHI *et al.*, 1988), the result $T_f = T_i$ at $\psi = 54.7°$ is a general one. Note that unless $T_\parallel = T_\perp$ (i.e. an isotropic distribution, which is only valid for low ion–neutral relative velocities), the measured T_f is not equal to T_i at any other angles.

The experiment was run from 0130 to 0430 UT on 16 December 1988. During the previous few hours, geomagnetic conditions had been very quiet, with an almost flat magnetogram trace at Kiruna. The K_p indices for the 12-h period preceding the event (1200–2400 UT on 15 December) were 1+, 1+, 1, 0+, but increased to 4−, 3 for the period 0000–0600 UT on 16 December: that activity was probably associated with the strong flows and ion heating event described in this paper.

The remote stations at Sodankylä (Finland) and Kiruna (Sweden) positioned the radar antennae so that their lines-of-sight intersected the Tromsø beam at an altitude of 275 km (geographic latitude = 72.0° and longitude = 19.21°), allowing an unambiguous, tristatic estimate of the bulk plasma flow (and hence electric field) with a basic time resolution of 10 s. A 390 μs pulse was transmitted from Tromsø, allowing range profiles of electron density and temperature, ion temperature and l-o-s velocity, with a range resolution of 58 km, to be measured. In addition, a shorter pulse (84 μs) was also transmitted, allowing profiles of electron density with a range resolution of 12.6 km to be obtained. For Kiruna and Sodankylä, the l-o-s temperature and bulk velocity measured are those for the bisector of the transmitter and receiver beams, i.e. at aspect angles of 61.69 and 62.6°, respectively.

The data analysis was performed using both a 'Maxwellian' and the semi-analytic 'non-Maxwellian' spectral synthesis routine given by SUVANTO (1988), which is based on the theoretical work of RAMAN *et al.* (1981). These workers used the form of distribution function derived theoretically for the relaxation model of ion–neutral collisions and an empirical correction to allow for shortcomings of this model: this correction includes replacing the ion drift Mach number, D', with a shape distortion parameter D^*. The fitting procedure used in this paper is described in detail by SUVANTO *et al.* (1989). LOCKWOOD and WINSER (1988) presented results obtained from this analysis, with Monte–Carlo simulations of the ion velocity distribution function for almost identical ionospheric conditions (KIKUCHI *et al.*, 1988), and concluded that the RAMAN *et al.* (1981) distribution function is a good first-order approximation to the real distribution function under such conditions. It should be noted that because observations are made at 54.7°, the ion temperature derived does not depend upon an assumed form for the three-dimensional ion velocity distribution function. All that is required is that the distribution of line-of-sight velocities at $\psi = 54.7°$ are able to reproduce the observed spectrum.

3. OBSERVATIONS

Figure 1 summarizes the observations from 16 December 1988 which were obtained using the experimental procedure described above. The top panel shows the magnitude of the bulk plasma flow at 275 km as a function of UT. Clearly for most of the period the velocity magnitude was in the range 500–800 m s^{-1}. The exception to this was the 15-min period between 0140 and 0155 when the velocity magnitude increased to about 4 km s^{-1}, corresponding to an electric field strength close to 200 mV m^{-1}. Panels (b)–(d) show the results of an analysis assuming the ion velocity distribution is always Maxwellian: the electron density was at its minimum value during the event while the ion temperature increased from 1400 to around 2700 K. The lowest panel illustrates that the electron temperature showed no clear response to the enhanced electric fields. This event is very characteristic of the formation of what are known as high-latitude troughs (WILLIAMS and JAIN, 1986; WINSER *et al.*, 1986; JONES *et al.*, 1990). This is better illustrated in Fig. 2, which shows the electron density and

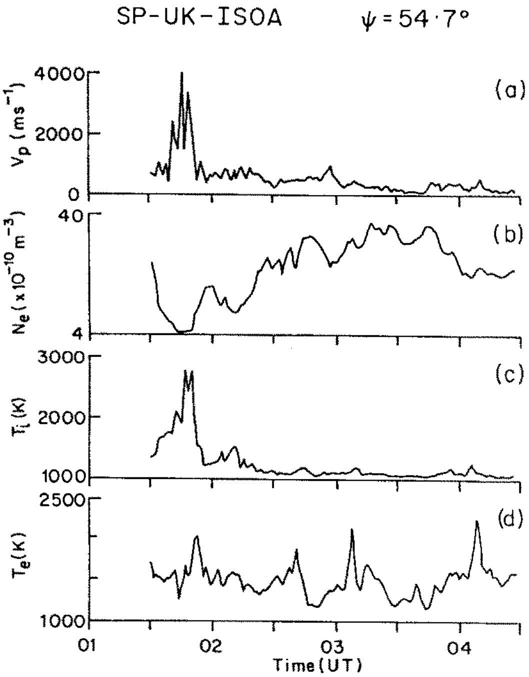

Fig. 1. Summary of plasma parameters for the period 0100–0430 UT on 16 December 1988, obtained using the U.K.–EISCAT special observing program ISOA. The aspect angle (ψ) for this experiment remained fixed at 54.7°, and the plasma parameters displayed in (b)–(d) were derived with the assumption that the line-of-sight distribution of ion velocities was Maxwellian. The bulk plasma velocity displayed in (a) was obtained by combining the components of velocity measured at the three radar sites in Tromsø, Kiruna and Sodankylä.

ion temperature observed along the Tromsø beam as a function of altitude and UT. The clear correlation between electron density depletion and ion temperature enhancement is evident; however, it should be noted that because the radar is looking due north at an elevation of 44° the observations at the greater altitudes are also further north. This figure clearly shows that the electron density trough was created locally (coincident with enhanced ion temperatures) and did not drift northward or southward across the radar field-of-view. This is an important consideration if a reasonable description of the ion chemistry is to be attempted (Section 7).

The absolute values for the electron density and plasma temperatures within the heating event should be treated with some caution in Figs 1 and 2, as this 'first-look' analysis was performed using the assumption of a Maxwellian ion velocity distribution. This is clearly an incorrect assumption under these large electric field conditions, and this point is discussed in more detail in the following sections.

4. NON-MAXWELLIAN ANALYSIS OF DATA

The incoherent scatter spectra are very different for the situations when the distribution of line-of-sight ion velocities are Maxwellian and highly non-Maxwellian. In the Maxwellian case, F-region spectra are the classic double-humped shape as described by Evans (1969), where the width is determined primarily by the ion temperature/mass ratio, and the separation of the peaks is defined by the electron/ion temperature ratio. In the non-Maxwellian case the situation is very different. The spectra generally become wider as a result of the broadening of the distribution function. The spectra also consist of a well-defined central peak with 'shoulders' near the frequency corresponding to the phase velocities of the up- and down-going ion acoustic waves. This peak arises from a decrease in the dielectric constant at low frequencies. These effects are very obvious from Fig. 3, which shows examples of the spectra observed at Tromsø and Kiruna during, and after, the event described in Fig. 1. In the case of the Tromsø spectra the non-Maxwellian effects are much less noticeable at higher altitudes due to the reduced number of ion–neutral collisions, and possibly because the drift was lower at the higher latitudes of these further range gates. The spectra observed at Kiruna during the event are considerably noisier than they are following the event (though the non-Maxwellian features are still fairly clear). This is a consequence of the fact that the electron density decreases considerably during the event resulting in a much poorer signal-to-nose ratio at the remote sites.

Individual spectra were integrated over 30 s, and were then fitted for electron density, electron temperature, ion temperature, and the non-Maxwellian distortion factor (N_e, T_e, T_i, D^*) using the algorithm described by Suvanto *et al.* (1989), which is based on the distribution function of Raman *et al.* (1981). Initially an ionosphere consisting of 100% O^+ ions at 275 km was assumed in the analysis, but this point is discussed in more detail in the following sections. It is only necessary to perform the non-Maxwellian analysis during the period when the electric fields were enhanced, and in the following discussion only data where good fits to the observed spectra were obtained are considered.

Figure 4a presents the derived ion temperature at the intersection scattering volume as a function of the square of the plasma velocity (V_p) for the period 0130–0200 UT. As expected from simple energy arguments there is a fairly clear linear relationship between the two parameters. Figure 4b shows a scatter plot of D^* against the bulk velocity magnitude for the same period. For the largest values of V_p the estimates for D^* approach the limit expected for a torus [$D^* \approx 1.25$ (ST-MAURICE and SCHUNK, 1979)], indicating the non-thermal nature of the plasma during this period. (However, the values shown assume that the ion gas remained purely O^+, which is extremely unlikely for these conditions. SUVANTO *et al.* (1989) showed that the non-Maxwellian analysis procedure used here would give a lower limit for $D^*(O^+)$ if molecular ions were also present.) Figure 4c indicates the clear anti-correlation between the electron density and the ion temperature, as expected when a high-latitude trough forms. If the electric field is very strong (as in this case) the electron density is so severely depressed that the signals measured at the remote sites are very noisy. This can result in large errors in the estimates of the convection velocities, which appears to be the source of the larger scatter in Fig. 4a and b. The data quality tends to be higher at Tromsø, and as the ion temperature can be used as a good tracer for the electric field, one would expect there to be a reasonable correlation between the ion temperature and D^*. This point is verified in Fig. 4d where D^* decreases to zero as the ion temperature approaches the neutral temperature. The derived electron temperature (not shown in Fig. 4) shows no strong dependence on the electric field strength.

Figure 5 summarizes the results of the non-Maxwellian analysis at the intersection height (275 km) for the period discussed in the previous paragraph. The top panel shows the derived plasma temperatures, with T_i clearly enhanced over T_e when the electric field is increased. Qualitatively this behaviour was apparent even for the Maxwellian analysis; however, because of the allowances for the distortion of the ion velocity distribution function from a Maxwellian, the derived ion temperature (for an assumed mass) should be more accurately determined. As the aspect angle for these observations was fixed at 54.7°, the derived ion temperature also corresponds to the true, three-dimensional temperature which can be used for energy considerations. WINSER *et al.* (1989) showed that analyzing such data with the assumption of a Maxwellian distribution function would lead to an overestimate of the ion temperature at large aspect angles, and an underestimate of the ion temperature at lower aspect angles. Also shown on this plot (using triangles) are the ion and electron temperatures derived from the analysis, which assumed a Maxwellian distribution function (refer to Fig. 1). Clearly both the 'Maxwellian' and 'non-Maxwellian' analysis produced temperatures which were in significant agreement before and after the heating event. However, the 'Maxwellian analysis' clearly overestimates the true ion temperature in the middle of the heating event by up to 300 K. The effect in the derived electron temperature is similar, but much less marked. The second panel in Fig. 5 shows the steady decrease and subsequent recovery of the electron density through the event. The lowest panel shows the variation of D^* (assuming the ion gas is O^+ ions) as a function of UT through the event, reiterating the clear correlation between D^* and T_i. We believe that these parameters are determined to a much greater degree of accuracy than they would have been if a Maxwellian velocity distribution had been assumed. In particular, the l-o-s ion temperature, T_f, has been derived with allowance for the non-Maxwellian nature of the distribution of l-o-s velocities, and because $\psi = 54.7°$, this is equal to the ion temperature, T_i, (which is a major factor in the energy balance equation) with no errors introduced by the anisotropy of the ion velocity distribution function. We now present a novel method to determine the ion mass using a combination of the ion energy equation and the results from the non-Maxwellian analysis described above.

5. ESTIMATES OF THE ION MASS FROM THE SIMPLE ION ENERGY EQUATION

The general form of the ion energy equation has been described previously by several authors (BANKS and KOCKARTS, 1973; ST-MAURICE and HANSON, 1982) and will not be described in any detail here. However, it is possible to simplify this equation by making certain assumptions, most notably that: heat advection and conduction terms are insignificant below about 400 km altitude; effects due to the partial differential with respect to time can be ignored, as we are only interested in events happening on a time-scale greater than the inverse of the ion–neutral collision frequency; the ion drift is non-divergent; and that no relative ion–electron drift exists at the height under discussion. The equation can then be written as:

$$T_i - T_n = \frac{\bar{m}_n}{3k}[V_p - V_n]^2 + \frac{m_i + m_n}{m_i}\frac{\nu_{ie}}{\nu_{in}}[T_e - T_i] \quad (3)$$

where V_n and T_n are the neutral wind velocity and temperature respectively; m_i and m_n are the ion and neutral masses; ν_{in} and ν_{ie} are the ion–neutral and ion–electron collision frequencies; and k is the Boltzmann constant.

According to equation (3), the temperature difference between the ions and neutral particles depends

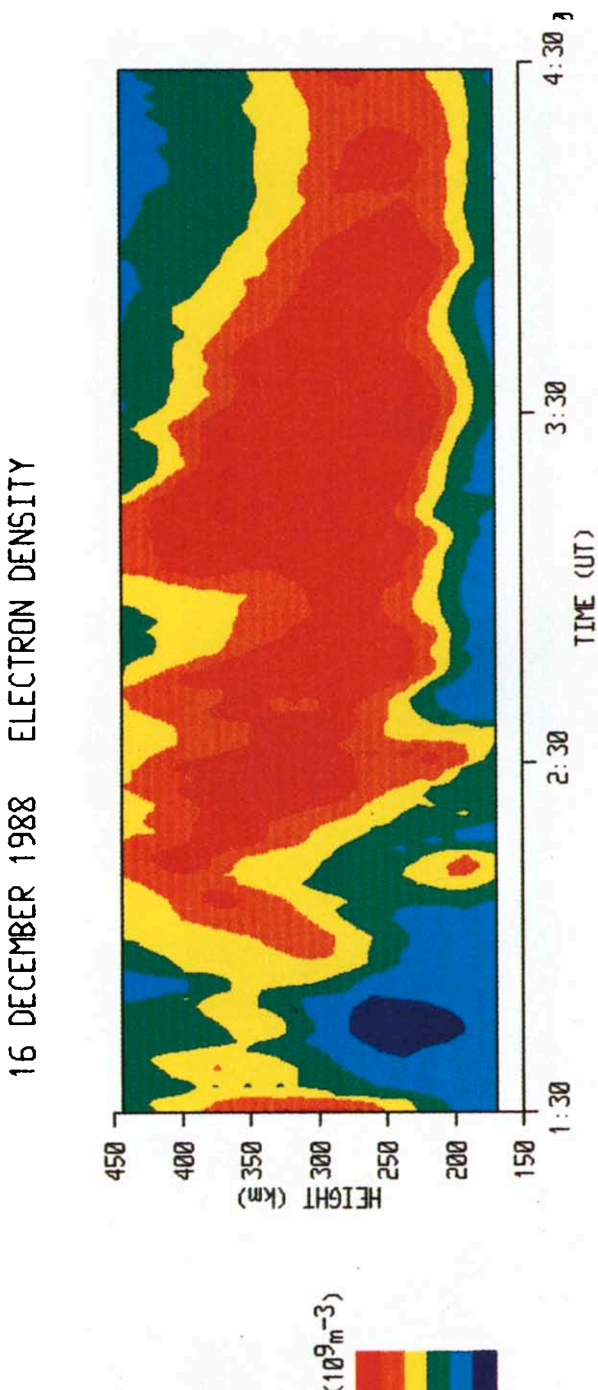
16 DECEMBER 1988 ELECTRON DENSITY
HEIGHT (km)
450
400
350
300
250
200
150
1:30
2:30
3:30
4:30
TIME (UT)
Ne (10^{9}m^{-3})
240
190
140
90
40

Fig. 2(a).

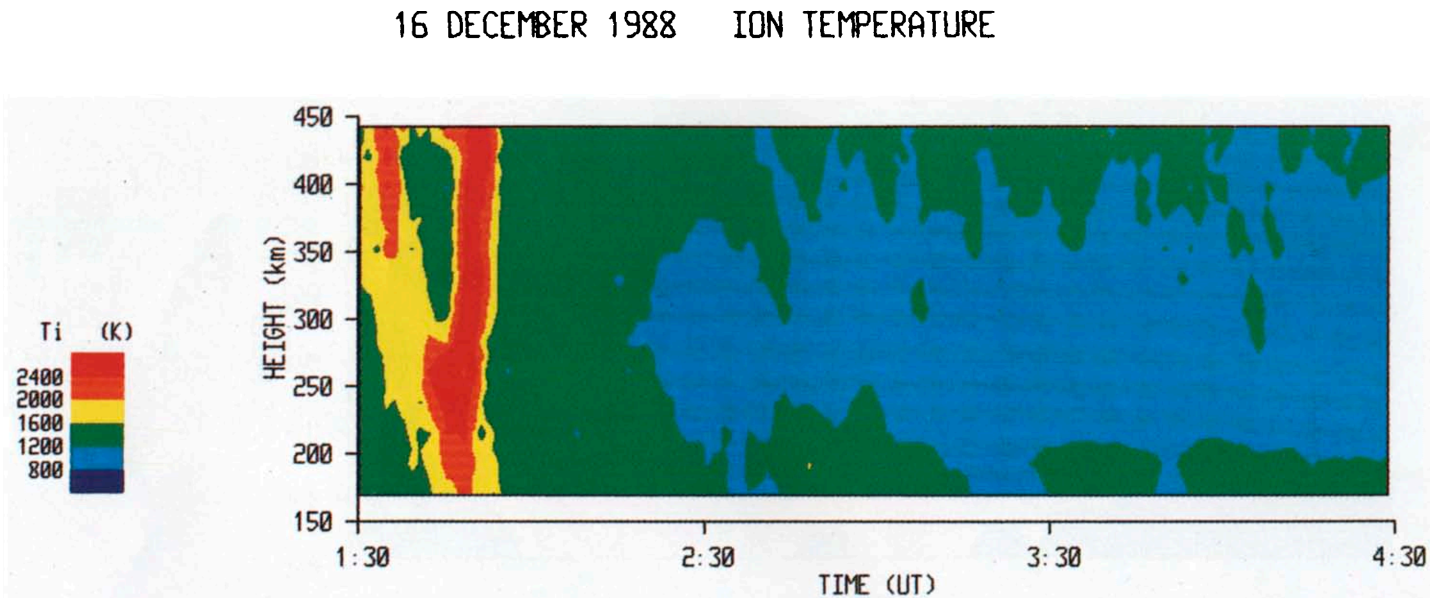

Fig. 2(b).

Fig. 2. Electron density (a) and ion temperature (b), from the 'Maxwellian' analysis, as a function of altitude and UT for the period described in Fig. 1. As the radar was pointing due north at an elevation of 44° during this period, the highest altitude measurements were made at a greater latitude than those at the lowest heights. The geographic latitude range covered in the plots is 70.9–74.0°.

upon frictional heating, and the heat exchange between ions and electrons. It is possible to use the plasma temperatures and convection velocities obtained from the radar, along with suitable models for the neutral wind and temperature, and the collision frequencies, to test the validity of using this simplified equation to model heating events such as that presented in Fig. 1. However, there are other factors which have to be considered when doing this. In addition to distorting the ion velocity distribution function from an isotropic Maxwellian, enhanced electric fields result in other processes which in turn affect the ion energy balance. The most obvious of these are: (1) the neutral atmosphere is accelerated by the ions, which reduces the frictional heating; (2) the neutral atmosphere is heated; (3) the composition of the neutral atmosphere changes; (4) the ion composition changes; (5) the electron density is depleted, which in turn affects the degree of ion–neutral coupling; (6) the ions are heated; and (7) plasma instabilities are produced. These processes can all occur simultaneously, but the time-scales for each of them can be different. The first three are not so important for the analysis which follows, as the event only lasts for 10–15 min, and this is less than the expected time-scales for these processes. The last of the effects (7) is very difficult to quantify and is currently a topic under study (SUVANTO, 1989). In any event it does not really affect the ion energy balance directly. The consequences of topics (4), (5) and (6) are the subject of the following discussion.

The width of the incoherent scatter spectrum is approximately proportional to the ion temperature/mass ratio (SALPETER, 1960; DOUGHERTY and FARLEY, 1963; EVANS, 1969), and so the values derived for the ion temperature depend critically on the as-

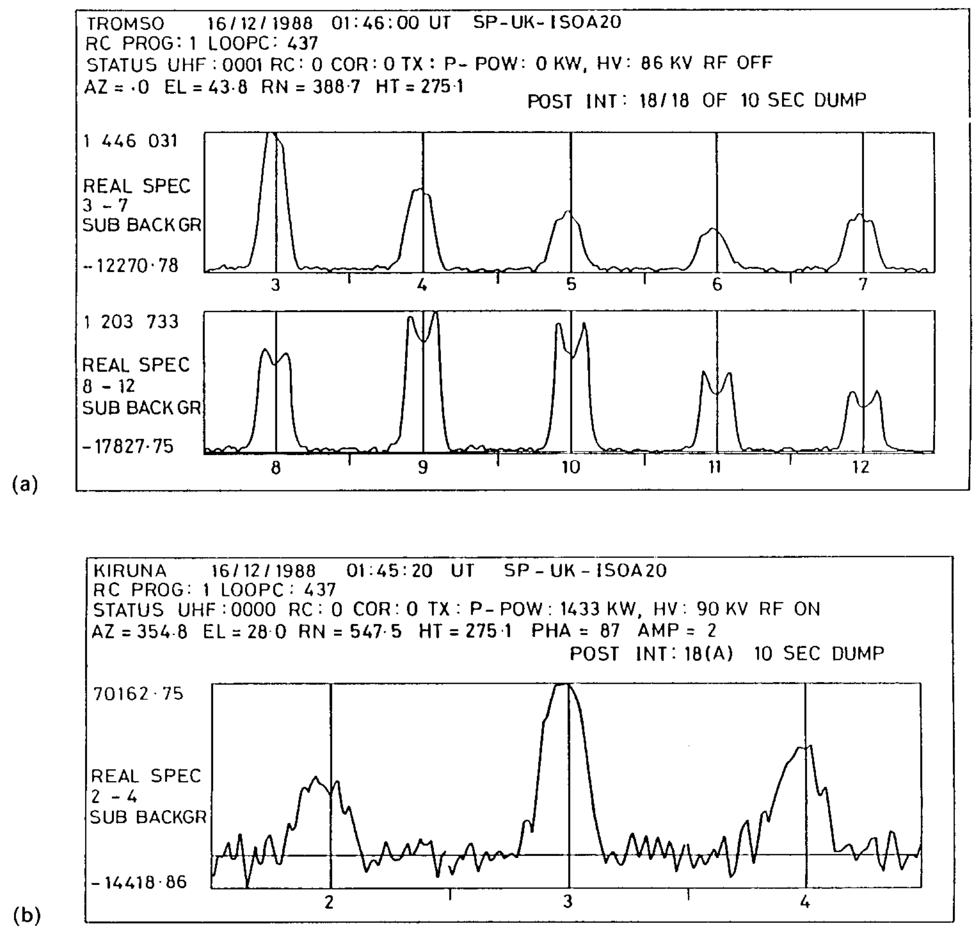

Fig. 3(a) and (b).

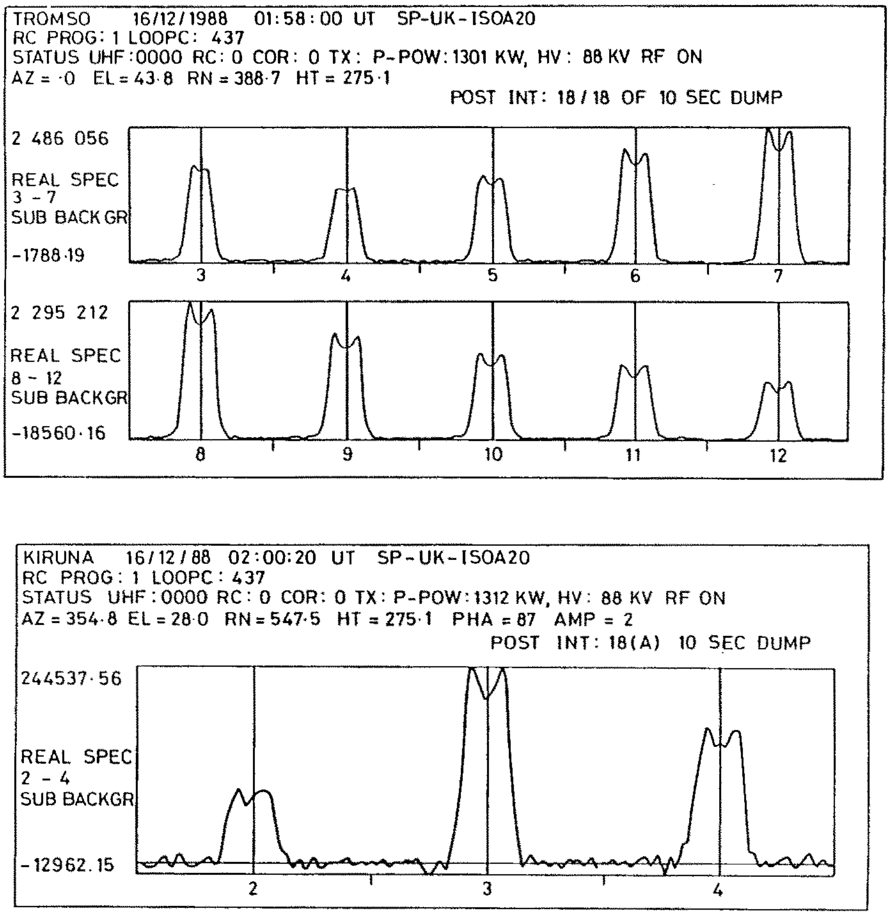

(c)

(d)

Fig. 3. (a) Incoherent scatter spectra as a function of range (gates 3–12) observed at Tromsø during the period when the plasma flows were around 3–4 km s^{-1} (see Fig. 1). The spectra have been integrated for 3 min but otherwise have not been processed or smoothed in any way. Panel (b) is similar to (a), but shows the spectra observed in the intersection volume by the Kiruna receiver. Figure 3(c) and (d) are similar to Fig. 3(a) and (b), respectively, but correspond to a period when the plasma velocity was relatively small ($\sim$600 m s^{-1}).

sumed ion mass (see, for example, KELLY and WICKWAR, 1981; LATHUILLERE *et al.*, 1983). In the analysis described in the preceding paragraphs, O^+ was assumed to be the only ion present at 275 km, though this is unlikely to be the case under the circumstances reported in this paper (see, for example, LATHUILLERE and BREKKE, 1985). WINSER *et al.* (1989) presented observations from a similar set of conditions and concluded that molecular ions, and in particular N_2^+, formed a major proportion of the ion population at 275 km. Their observations were unusual in the respect that NO^+ is usually assumed to be the dominant molecular ion in the lower *F*-region. We have adopted a novel approach to use the single species analysis in conjunction with the ion temperature derived from the simplified form of the ion energy equation to estimate the real ion mass as a function of time throughout the event. From the non-Maxwellian analysis we find that the ratio of the derived ion temperature (T_i) over the assumed ion mass (m_i) is constant to within about 20% (see Fig. 7). To a first approximation we can then state that:

$$\frac{T_i(\text{analysis})}{m_i(\text{assumed})} \approx \frac{T_i(\text{real})}{m_i(\text{real})} \tag{4}$$

where T_i(analysis) is the ion temperature derived from the non-Maxwellian analysis for an assumed ion mass, m_i(assumed). T_i(real) and m_i(real) are the real ion tem-

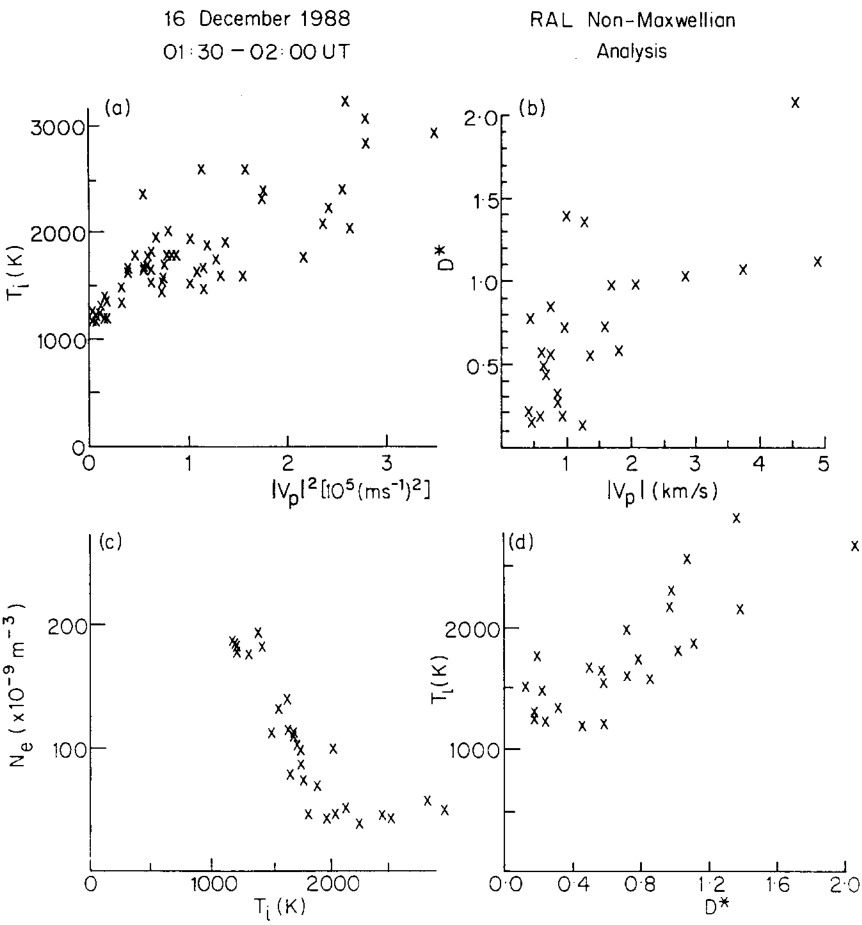

Fig. 4. Results of a single-species (O^+) non-Maxwellian analysis of the data obtained in the period 0130–0200 UT on 16 December at Tromsø. The raw data in this case were post-integrated for 30 s, and only data where the analysis succeeded in obtaining a satisfactory fit to the measured spectra are presented. The figure shows scatter plots of: (a) ion temperature against the square of the bulk plasma velocity; (b) the derived non-Maxwellian shape distortion parameter (D^*) vs the magnitude of the bulk plasma flow; (c) the measured electron density as a function of ion temperature; and (d) the derived ion temperature as a function of D^*.

perature and mass, respectively. It is now possible to solve equation (3) for T_i(real) and substitute this value into equation (4) to solve for m_i(real). Neglecting the ion–electron conduction term in (3) yields:

$$m_i(\text{real}) = \frac{T_n}{T_i(\text{analysis})} \times \left[1 + \frac{m_n[V_p - V_n]^2}{3kT_n}\right] m_i(\text{assumed}). \quad (5)$$

The validity of this assumption will be discussed later.

It is necessary to make estimates of the neutral wind and temperature to solve this equation for m_i(real). The value for the neutral temperature was taken to be the same as the measured ion temperature between 0300 and 0400 UT when the electric fields were small. This value was consistent with MSIS86 model predictions of T_n for similar location and conditions. From the MSIS86 model, it may also be deduced that, before the event, the horizontal pressure gradient in the neutral air, acting in conjunction with Coriolis force and ion drag, would drive a wind of about 50 m s^{-1}, approximately in the north–south direction. This is smaller than the ion drift observed at the start of the event, and would not greatly affect the ion heating as deduced from equation (3). The small magnitude of the wind is consistent with the very quiet

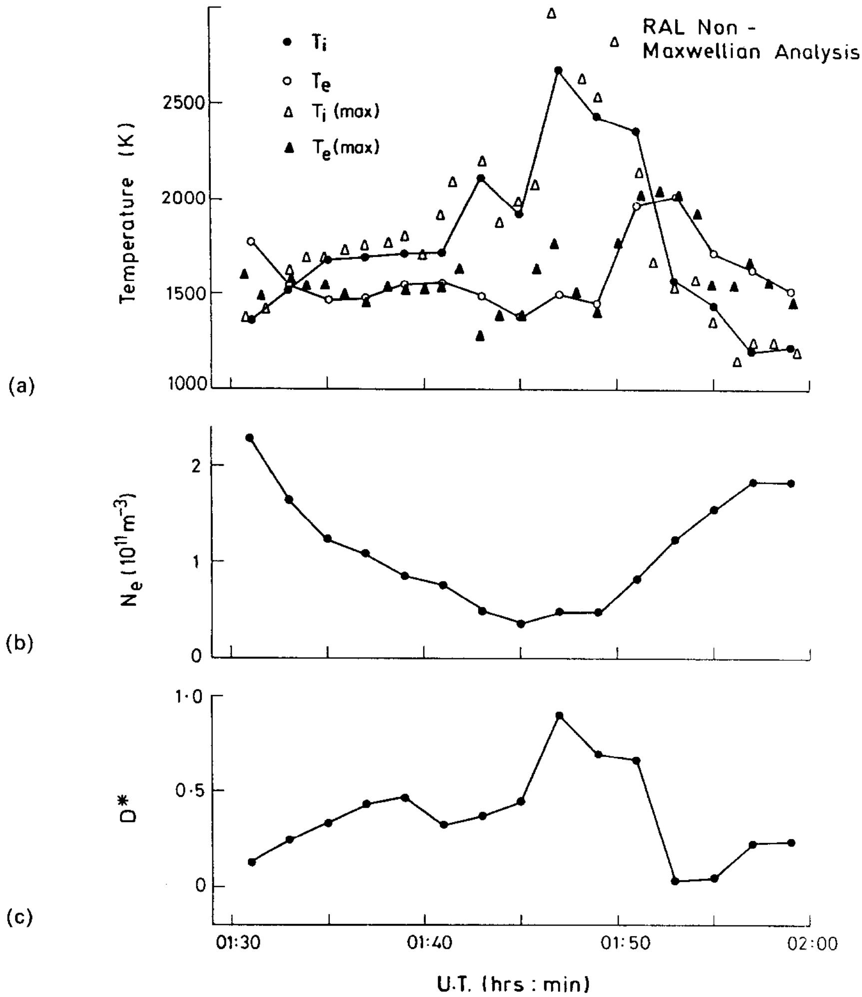

Fig. 5. Summary of the plasma parameters as a function of UT for the period described in Fig. 4. These parameters result from the single-species, non-Maxwellian analysis described in Section 4. Figure 5(a) shows the derived ion temperature (solid circles) and electron temperature (open circles). [Also shown are the ion (open triangles) and electron (solid triangles) temperatures from the Maxwellian analysis presented in Fig. 1.] Panel (b) shows the derived electron density, and (c) the non-Maxwellian shape distortion parameter (D^*). The data in this figure, resulting from the non-Maxwellian analysis, have been post-integrated for 2 min.

magnetic conditions prevailing prior to the intense heating. We have also assumed that the magnitude of the neutral wind did not change through the event, which only lasted for about 15 min. This is considerably smaller than the estimated time-scale for the neutral wind to respond to the rapid change in plasma flow, considering the electron densities measured at the time. If, however, the wind were to change by a factor of 2 or 3 during the heating event, this would still be a very small factor (compared with the very large increase in ion velocity) in the calculations of the ion mass using equation (5). The results of these calculations are presented in Fig. 6.

The top panel (a) shows the two components of the plasma flow perpendicular to the geomagnetic field, V_{pN} and V_{pE}. These data have been averaged for 2 min in an attempt to reduce the errors in the derived velocities caused by the poor signal-to-noise ratio at the remote sites during the event. For shorter post-integration periods, the errors in V_{pN} and V_{pE} provide the largest source of error in the calculations of m_i(real) described below. The second panel (b) reproduces the ion temperature derived from the non-Maxwellian

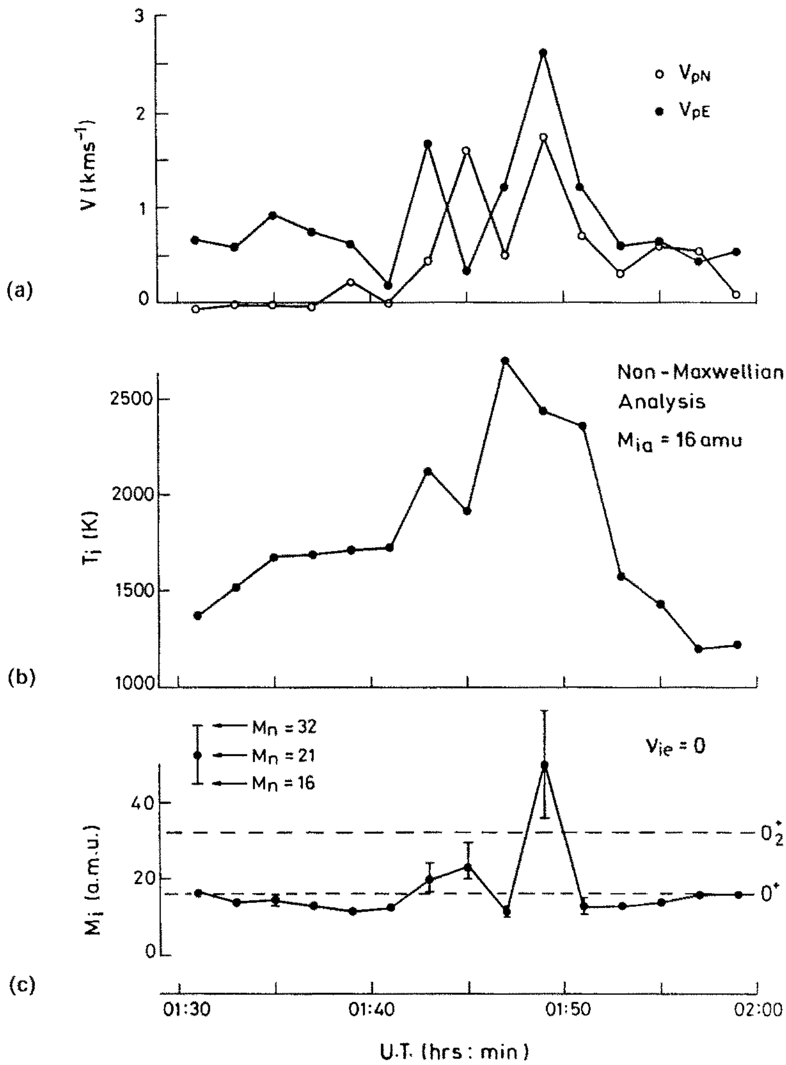

Fig. 6. The top panel shows the eastward (solid circles) and northward (open circles) components (with respect to the geomagnetic field) of the bulk plasma flow for the period 0130–0200 UT on 16 December. The middle panel (b) shows the corresponding ion temperature derived from a single-species non-Maxwellian analysis of the data (the same as that presented as part of Fig. 5(a)). The lower panel (c) illustrates the calculated ion mass as a function of UT, assuming the ion temperature/mass ratio to be constant. The error bars correspond to the range of values obtained for an assumed neutral mass between 16 and 32 a.m.u. The horizontal dashed lines correspond to the mass of O^+ and NO^+ (or O_2^+) for the lower and upper lines, respectively. These calculations neglect heat exchange between ions and electrons in the simple ion energy balance equation.

analysis described above (refer to top panel in Fig. 5). This corresponds to T_i(analysis) in equation (5) [for m_i(assumed) of 16 a.m.u.] and shows a clear enhancement associated with the increased plasma flows in Fig. 6a. Figure 6c shows the estimated values for m_i(real) using equation (5). The derived values correspond to oxygen ions at the beginning and end of the period, but slowly decrease to about 13 a.m.u. until 0140, and then increase to around 25 a.m.u. at 0145 followed by another decrease. There is then a rapid increase to a value in excess of 40 a.m.u. followed by an equally sudden decrease at 0151. The ion mass slowly recovers to 16 a.m.u. at the end of the period.

There are several points which should be made about this figure. First, the error bars correspond to the range of values for m_i(real) obtained when the mean neutral mass, m_n, assumed in equation (5) varied between 16 and 32 a.m.u. (the solid circles correspond to an assumed neutral mass of 21 a.m.u., which is consistent with MSIS86 model predictions at this time). Second, the derived ion masses appear to be too low (13 a.m.u.) in the periods immediately before and after the event, but too high (48 a.m.u.) in the middle of the event. Firstly, we investigate the effects of neglecting ion–electron conduction as a possible cause of these inconsistencies. Reference to Fig. 5 shows that between 0133 and 0152 UT, T_i was elevated above T_e, with the largest difference occurring near the time when the bulk plasma flow was largest. Outside this period the electron temperature was larger than the corresponding ion temperature. Inclusion of this term in equation (5) would act to reduce the estimates of m_i(real) during the event (with the largest reduction occurring for the greatest ion–electron temperature difference), while increasing the estimates outside the heating event where $T_e > T_i$. However, simple calculations using expressions for ν_{in} (SCHUNK and NAGY, 1980) and ν_{ie} (RISHBETH and GARRIOTT, 1969) show that this term is insignificant in magnitude throughout the period of interest in this paper, accounting for less than 0.25 a.m.u. (maximum) in the calculated values of m_i(real). The largest sources of error in our calculations of m_i(real) result from (i) the uncertainties in the bulk ion flows due to the reduced signal-to-noise (particularly at the remote sites) during the heating event and, to a lesser extent, (ii) the estimate of the neutral wind. The latter effect is more important when the ion flows are small (i.e. outside the main heating period).

Even allowing for all these sources of error one conclusion can still be drawn from the calculations; namely, that the ion composition at 275 km altitude changed from predominantly oxygen to predominantly molecular ions over a period of a few minutes, in response to a sudden increase in the bulk plasma flow from several hundred metres per second to around 3–4 km s^{-1}.

6. MIXED SPECIES NON-MAXWELLIAN ANALYSIS

From the above discussion it is clear that the ion composition did not remain totally O^+ during the event described above. It therefore seems pertinent to re-analyze the data using the non-Maxwellian algorithm, but allowing for the possibility of a mixed species plasma. Under normal circumstances it would be necessary to fit for seven parameters from the observed spectra to describe adequately the plasma. These are: electron density, electron temperature, line-of-sight (l-o-s) ion temperature for both species considered [$T_f(O^+)$ and $T_f(NO^+)$], ion composition, and the non-Maxwellian shape distortion parameter for both species [$D^*(O^+)$ and $D^*(NO^+)$]. Recent attempts to fit this many parameters from the spectra have shown that the fits obtained are ambiguous (SUVANTO *et al.*, 1989). Because the anisotropy of the ion velocity distribution function will be different for atomic and molecular species, derived l-o-s temperatures, T_f, for the two species would be different at a general aspect angle, ψ. However, because the aspect angle for the experiment described here remained fixed at 54.7°, it is known that, to a very good approximation $T_f(O^+) = T_f(NO^+) = T_i$ (LATHUILLERE and HUBERT, 1989). Also, rather than trying to fit for ion composition, we have adopted the approach of fixing the composition at some predetermined value, attempting a five parameter fit [N_e, T_e, T_i, $D^*(O^+)$, $D^*(NO^+)$], then repeating the exercise again for a different value of composition, and searching for a minimum in the fit variance. This reduces the number of fit parameters to five, which WINSER *et al.* (1989) and SUVANTO *et al.* (1989) have shown to be a reasonable number.

Figure 7 is an example of the results from the mixed-species, non-Maxwellian analysis for the data integrated over the period 014900–014930. The top panel shows the derived plasma temperatures as a function of assumed ion composition. This illustrates very clearly the dependence of the derived temperatures on the assumed ion mass, with a difference of around 2000 K in both electron and ion temperature between a pure O^+ and pure NO^+ plasma. Such behaviour has been observed previously in cases where a Maxwellian ion velocity distribution has been assumed (KELLY and WICKWAR, 1981; LATHUILLERE *et al.*, 1983). The first of these authors estimated the ion mass by assuming model electron temperature profiles, and applying a full least-squares fit of a theoretical autocorrelation function (ACF) to the measured function. This method was also used successfully at lower latitudes where the ion temperature was assumed to be the same as the neutral temperature (MOORCROFT, 1964; EVANS and COX, 1970; WAND and PERKINS, 1970; ALCAYDE *et al.*, 1974). LATHUILLERE *et al.* (1983) used a method to estimate the ion mass which was closer to the method described in this paper. They attempted several fits on the measured ACF with fixed composition ranging from 100% molecular ions to purely atomic ions, and used the minimum variance from the fits to indicate when the derived ionospheric

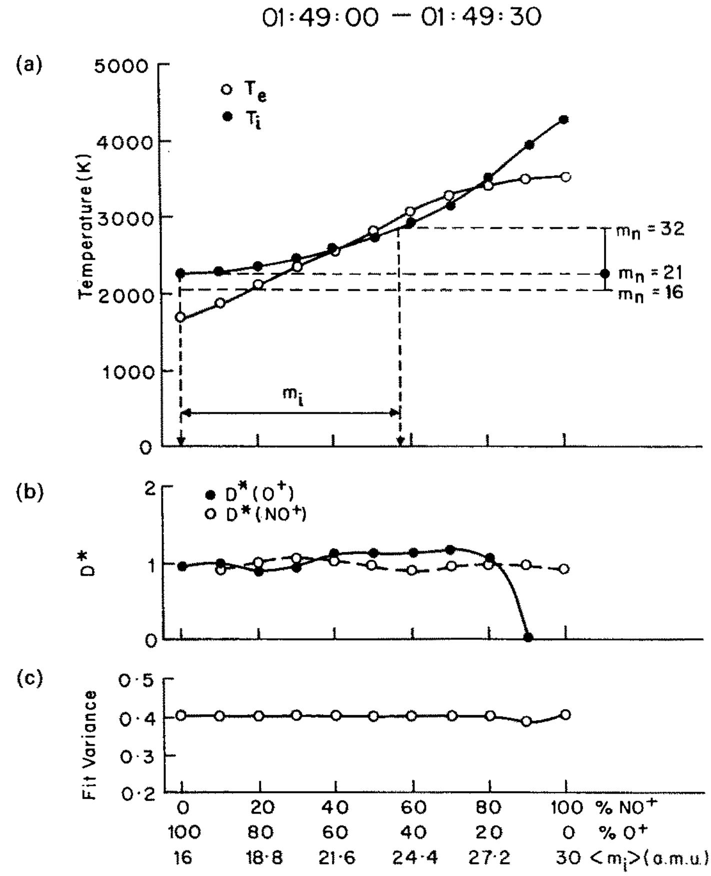

Fig. 7. Results from a five parameter (mixed species) fit to the data integrated over the period 014900–014930 on 16 December. Each point on the curves correspond to the results of an analysis with the ion mass assumed (shown on the abscissa). The point (solid circle) on the right-hand side of the top panel corresponds to the ion temperature [T_i(real)] derived using the simplified form of the ion energy equation, and the error bar corresponds to the range of values obtained for an assumed mean neutral mass between 16 and 32 a.m.u. The dashed lines represent the projection of this estimate of ion temperature onto the ion temperature/ion mass curve obtained from the mixed-species, non-Maxwellian analysis, and hence allow a range of ion masses at this time to be evaluated.

parameters were closest to the final solution. They then used these parameters as initial values for a full fit (including ion composition) on the measured ACF. We believe that this is more reliable than the method described by Kelly and Wickwar (1981) for interpreting data obtained at high latitudes, where intense ion and electron heating (which may vary rapidly with time) are commonly observed.

Figure 7 also indicates that the ion temperature/mass ratio (T_i/m_i) remains fairly constant for these data, changing by 20% in the extreme case. This is consistent with previous findings (Suvanto *et al.*, 1989; Winser *et al.*, 1989; Lockwood *et al.*, 1989) and justifies the use of equation (4). Figure 7b shows the fitted D^* values for both the atomic and molecular ions. Both $D^*(O^+)$ and $D^*(NO^+)$ are about 1.0 for all values of ion composition. This is a little surprising as the collision mechanisms for NO^+ are not really conducive to producing toroidal ion velocity distributions. However, the lower panel shows that the fits were insensitive to ion composition in this case, with no discernable minimum in the variance curve for any given composition.

Ths solid circle (with the error bar) on the right-hand side of Fig. 7a is the value of the ion temperature [T_i(real)], derived from the simplified ion–energy equation for this period. The error bar corresponds to the range of values obtained for an assumed mean

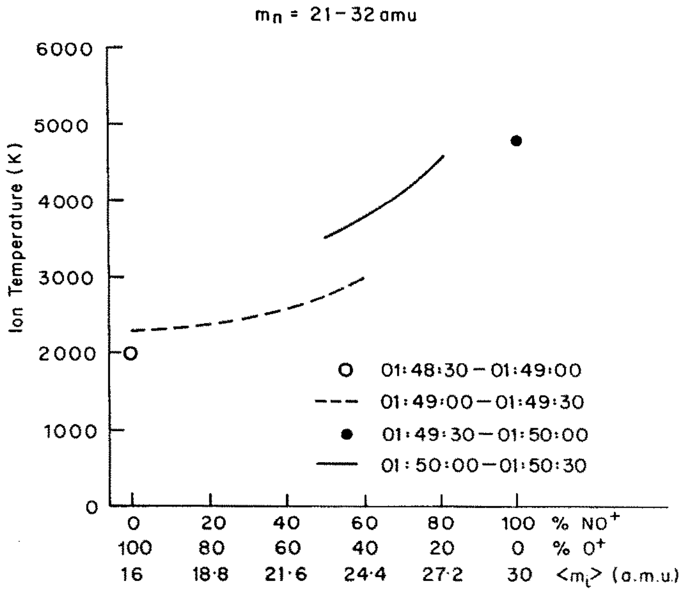

Fig. 8. Sections of the ion temperature against assumed mass curves (from mixed-species, non-Maxwellian analysis) corresponding to the projections of the ion temperatures calculated using the simplified form of the ion energy equation for four periods as shown. Each point or section corresponds to a 30-s post-integration, and the 2-min period covered in this figure covers the peak of the ion heating event discussed in the text.

neutral mass between 16 and 32 a.m.u. From this estimate of T_i(real) it is possible to infer (by interpolation) the corresponding ion composition from the ion temperature/ion mass curve, derived from the mixed-species, non-Maxwellian fits to the data. This procedure was repeated for several integration periods through the peak of the heating event, and the results are summarized in Fig. 8, which shows the ion composition corresponding to the estimates of T_i(real) for the four 30-s integrations in the period 014830–015030. This period covers the peak estimated value for m_i(real) as described in the previous section. The plot shows a clear increase from 100% O^+ to 100% molecular ions as the temperature increases due to the enhanced electric fields, and similarly a decrease in the ion mass as the temperature falls again. From this plot it is possible to estimate that the ion mass changes from O^+ to NO^+ ions at an approximate rate of 1% change in the mean ion mass per 26 K of ion temperature for the event described in this paper. It is also fairly clear from Fig. 7 that $m_n = 21$ a.m.u. represents a minimum value for the neutral mass during the heating event.

7. ION COMPOSITION DURING THE HEATING EVENT

According to the standard theory of the F-region (e.g. RISHBETH and GARRIOTT, 1969, section 3.61), the molecular/atomic ion concentration ratio depends on the relative rates of the ion–molecular transfer reactions (characterized by the linear loss coefficient β) and the subsequent dissociative recombination reaction (characterized by the square-law coefficient α), of which the most important are probably:

$$O^+ + O_2 \rightarrow O_2^+ + O \quad \text{(rate coefficient } K_1\text{)} \tag{6a}$$

$$O^+ + N_2 \rightarrow NO^+ + N \quad \text{(rate coefficient } K_2\text{)} \tag{6b}$$

$$O_2^+ + e \rightarrow O + O \quad \text{(rate coefficient } \alpha_1\text{)} \tag{7a}$$

$$NO^+ + e \rightarrow N + O \quad \text{(rate coefficient } \alpha_2\text{).} \tag{7b}$$

In a steady-state photochemical situation, to which the lower $F2$-layer normally approximates, the molecular/atomic ion ratio is given by

$$r = \beta/\alpha N = \{K_1 n[O_2] + K_2 n[N_2]\}/\alpha N \tag{8}$$

where $n[X]$ denotes the concentration of the neutral gas X, and α is a combination of α_1 and α_2, which in our experiment we may take to be their mean (since α_1 and α_2 are found to differ by only 20%).

Estimates of the parameters, taken from appendix 5 of REES (1989) and converted to m.k.s. units, are as follows:

$$K_1 = 2.0 \times 10^{-17}(T_r/300)^{-0.4}\,\mathrm{m^3\,s^{-1}} \tag{9a}$$

$$K_2 = 4.5 \times 10^{-20}(T_r/300)^2\,\mathrm{m^3\,s^{-1}} \tag{9b}$$

$$\alpha_1 = 1.9 \times 10^{-13}(T_r/300)^{-0.5}\,\mathrm{m^3\,s^{-1}} \quad (9c)$$

$$\alpha_2 = 4.2 \times 10^{-13}(T_r/300)^{-0.85}\,\mathrm{m^3\,s^{-1}} \quad (9d)$$

where T_r is the 'reduced temperature' $(T_n + T_i)/2$. Taking values of atmospheric parameters from the MSIS86 model (HEDIN, 1987) for the date, place and time of the heating event, we have $n[\mathrm{O_2}] = 2.8 \times 10^{13}\,\mathrm{m^{-3}}$, $n[\mathrm{N_2}] = 5 \times 10^{14}\,\mathrm{m^{-3}}$ and gas temperature $T_n = 1200\,\mathrm{K}$. We assume that these parameters do not change significantly during and after the 15-min heating event, which seems reasonable (unless there was strong Joule heating by a nearby auroral electrojet, which does not seem consistent with the small disturbance of $< 100\,\mathrm{nT}$ of the Kiruna magnetogram). From the data we have that during the event (0148 UT):

$$N_e = 0.4 \times 10^{11}\,\mathrm{m^{-3}}, \quad T_i = 2500\,\mathrm{K}, \quad T_r = 1850\,\mathrm{K},$$

$$T_e = 1500\,\mathrm{K}, \quad \alpha = 0.95 \times 10^{-13}\,\mathrm{m^3\,s^{-1}}$$

whence:

$$\beta = \beta_1 + \beta_2 = (0.27 + 0.85) \times 10^{-3}\,\mathrm{s^{-1}}$$

$$= 1.12 \times 10^{-3}\,\mathrm{s^{-1}}, \quad \alpha N_e = 3.8 \times 10^{-3}\,\mathrm{s^{-1}}$$

so that from equation (8) $r = 0.3$ (i.e. 23% molecular ions).

After the event (say, 0200 UT onwards):

$$N_e = 2.0 \times 10^{11}\,\mathrm{m^{-3}}, \quad T_i = 1200\,\mathrm{K}, \quad T_r = 1200\,\mathrm{K},$$

$$T_e = 1500\,\mathrm{K}, \quad \alpha = 0.95 \times 10^{-13}\,\mathrm{m^3\,s^{-1}}$$

whence:

$$\beta = \beta_1 + \beta_2 = (0.32 + 0.36) \times 10^{-3}\,\mathrm{s^{-1}}$$

$$= 0.68 \times 10^{-3}\,\mathrm{s^{-1}}, \quad \alpha N_e = 1.9 \times 10^{-2}\,\mathrm{s^{-1}}$$

so that from equation (8) $r = 0.035$ (i.e. 3.5% molecular ions).

According to this calculation, the ninefold difference between the 'during-the-event' and 'after-the-event' values of the molecular/atomic ratio r is mainly due to the fivefold change in N_e. The change in the loss coefficient β does contribute, but not as much as might have been expected; this is because the large change in β_2 [due to the temperature dependence of the rate coefficient K_2, equation (6b)] is partly offset by the opposite temperature dependence of K_1, equation (6a). Of course, these coefficients are still not well known for the physical conditions encountered in the heating event, nor can we be sure of the neutral air composition, though we can at least rely on the MSIS86 value of T_n, since it agrees well with the observed values of T_i after the heating event. We are left with some difficulties:

(1) Despite the order-of-magnitude difference in our computed values of the ratio r, during and after the heating event, the value of $r = 0.3$ during the event disagrees with our observation of a predominantly molecular ion plasma at that time. We could perhaps try to increase this estimated value by a factor of 10 to give $r = 3$, say, which corresponds to 75% molecular ions and 25% atomic ions. Conceivably, this could be done by (a) raising the $\mathrm{N_2}$ concentration, (b) assuming a stronger temperature dependence of K_2, or (c) postulating an additional loss mechanism for $\mathrm{O^+}$ ions, possibly involving an excited state.

(2) The time constant for conversion of $\mathrm{O^+}$ ions to molecular ions is $1/\beta$ which, for the estimated values during the heating event, is 900 s. This is too long to account for the rapid observed change of ion composition, which again suggests that the estimated β is too small.

(3) On the other hand, increasing the loss coefficient β aggravates the difficulty of explaining the survival and subsequent recovery of the plasma. This difficulty is particularly severe if the ions are predominantly molecular, in which case their mean lifetime is approximately $1/2\alpha N$, which is only about 2 min during the event.

(4) If there is a rapid upwelling of the neutral air during the event, this would increase the molecular gas concentrations, and therefore increase r in equation (8). Doubling the $\mathrm{N_2}$ and $\mathrm{O_2}$ concentrations at 275 km height would go some way to meeting our difficulty about ion composition, but considering that there was not a strong auroral disturbance at the time the question of whether such a large change could occur within a few minutes needs further study. Upward transport of ions (rather than neutrals) seems unlikely to explain the change of ion composition, since molecular ions would only move a few kilometres during their lifetime, even with an upward velocity as large as $50\,\mathrm{m\,s^{-1}}$.

(5) The problem of plasma lifetime is related to the more general question of how the *F*-layer ionization is maintained during the winter night. At this time, when direct solar photoionization is absent, sources of ionizing radiation in the night sky are problematical, and there is no obvious steady source of particle precipitation; furthermore, the lack of any increase in electron temperature suggests that particle precipitation was not strong. The lifetimes just quoted imply that the plasma has to be completely replaced every few minutes (and this requirement becomes only slightly less stringent during the quiet period after the heating event).

These difficulties might be reduced (though probably not removed) if we could show that horizontal transport provides a significant source. However, a preliminary study of data from the other radar gates, i.e. neighbouring latitudes (Fig. 2), does not suggest that the depletion during the ion heating event moved systematically across the experiment's field-of-view. Other possibilities include downward diffusion from the protonosphere. To investigate this problem, further studies are needed of the velocity data.

8. CONCLUSIONS

Results are presented from an experiment where the aspect angle for the Tromsø beam remained fixed at 54.7°, allowing direct measurements of the true, three-dimensional ion temperature that can be used in energy balance arguments. During one set of observations the bulk plasma flows were observed to increase from a few hundred metres per second to around 4 km s^{-1} within a few minutes, resulting in enhanced ion temperatures and depleted electron densities. The spectra observed simultaneously at Tromsø and the remote sites clearly exhibit a form which is consistent with a distortion of the distribution of line-of-sight ion velocities from a Maxwellian. These data were analyzed using the semi-analytic spectral synthesis algorithm of SUVANTO (1988), which was based on the generalized form of the relaxation model of ion–neutral collisions described by RAMAN *et al.* (1981). This confirmed that the plasma was highly distorted from Maxwellian when the convection speeds were several km s^{-1}.

We have used the ion temperatures derived from the single-species, non-Maxwellian analysis, in conjunction with the simplified form of the ion energy balance equation, to calculate the ion mass during an intense ion heating event. This showed that the plasma at 275 km changed from predominantly O^+ to predominantly molecular ions within 2–3 min, in response to the enhanced ion temperatures caused by the rapid increase in convection electric field. If we neglect the heat exchange between ions and electrons in the ion energy equation, we underestimate the ion mass outside the heating event, but overestimate the ion mass at times when the ion temperature significantly exceeds the electron temperature. This effect, however, is a minor one and cannot easily explain the unusually large ion mass estimated using equation (5).

Results from a mixed-species, non-Maxwellian analysis confirmed the conclusion regarding the composition changes during large electric fields. We used these results in conjunction with the ion energy equation to quantify the dependence of ion composition on measured ion temperature for the event described in this paper. A theoretical consideration of the ion composition, using recently published values of the chemical rate coefficients in conjunction with the MSIS86 model, could explain an order of magnitude increase in the atomic/molecular ion ratio during the event, but could not explain the high proportion of molecular ions that were observed.

Acknowledgements—We are indebted to the Director and staff of EISCAT for operating the facility. EISCAT is an International Association supported by the research councils of Finland (SA), France (CNRS), the Federal Republic of Germany (MPG), Norway (NAVF), Sweden (NFR), and the United Kingdom (SERC). We acknowledge J.-P. St-Maurice and D. Hubert for providing stimulating discussions on various aspects of this work. GOLJ and MGA are grateful for financial support from the SERC during the period when this work was carried out.

REFERENCES

ALCAYDE D., BAUER P. and FONTANARI J. 1974 *J. geophys Res.* **79**, 629.
BANKS P. M. and KOCKARTS G. 1973 *Aeronomy* (parts A and B). Academic Press, New York.
DOUGHERTY J. P. and FARLEY D. T. 1963 *J. geophys Res.* **68**, 5473.
EVANS J. V. 1969 *Proc. IEEE* **57**, 496.
EVANS J. V. and COX L. P. 1970 *J. geophys Res.* **75**, 159.
HEDIN A. E. 1987 *J. geophys Res.* **92**, 4649.
HUBERT D. 1984 *J. atmos. terr. Phys.* **46**, 601.
JONES G. O. L., WILLIAMS P. J. S., WINSER K. J. and LOCKWOOD M. 1990 *Adv. Space Res.* **10**(6), 191.
KELLY J. and WICKWAR V. B. 1981 *J. geophys Res.* **86**, 7617.
KIKUCHI K., ST-MAURICE J.-P. and BARAKAT A. R. 1988 *Ann. Geophys.* **7**, 183.
LATHUILLERE C. and BREKKE A. 1985 *Ann. Geophys.* **3**, 557.
LATHUILLERE C. and HUBERT D. 1989 *Ann. Geophys.* **7**, 285.
LATHUILLERE C., LEJEUNE G. and KOFMAN W. 1983 *Radio Sci.* **18**, 887.
LOCKWOOD M., BROMAGE B. J. I., HORNE R. B., ST-MAURICE J.-P., WILLIS D. M. and COWLEY S. W. H. 1987 *Geophys. Res. Lett.* **14**, 111.

LOCKWOOD M., SUVANTO K., WINSER K. J., COWLEY S. W. H. and WILLIS D. M. 1989 *Adv. Space Res.* **9**(5), 113.
LOCKWOOD M. and WINSER K. J. 1988 *Planet. Space Sci.* **36,** 1295.
LØVHAUG U. P. and FLÅ T. 1986 *J. atmos. terr. Phys.* **48,** 959.
MOORCROFT D. R. 1964 *J. geophys. Res.* **69,** 955.
MOORCROFT D. R. and SCHLEGEL K. 1988 *J. atmos. terr. Phys.* **50,** 455.
PERRAUT S., BREKKE A., BARON M. and HUBERT D. 1984 *J. atmos. terr. Phys.* **46,** 531.
RAMAN R. S. V., ST-MAURICE J.-P. and ONG R. S. B. 1981 *J. geophys Res.* **86,** 4751.
REES M. H. 1989 *Physics and Chemistry of the Upper Atmosphere.* Cambridge University Press, Cambridge.
RISHBETH H. and GARRIOTT O. K. 1969 *Introduction to Ionospheric Physics.* Academic Press, New York.
SALPETER E. E. 1960 *Phys. Rev.* **120,** 1528.
SCHUNK R. W. and NAGY A. F. 1980 *Rev. Geophys. Space Phys.* **18,** 813.
ST-MAURICE J.-P. and HANSON W. B. 1982 *J. geophys. Res.* **87,** 7580.
ST-MAURICE J.-P. and SCHUNK R. W. 1979 *Rev. Geophys. Space Phys.* **17,** 99.
SUVANTO K. 1988 *Radio Sci.* **23,** 989.
SUVANTO K. 1989 *Planet. Space Sci.* **37,** 1.
SUVANTO K., LOCKWOOD M., WINSER K. J., BROMAGE B. J. I. and FARMER A. D. 1989 *J. atmos. terr. Phys.* **51,** 483.
WAND R. H. and PERKINS F. W. 1970 *J. atmos. terr. Phys.* **32,** 1921.
WILLIAMS P. J. S. and JAIN A. R. 1986 *J. atmos. terr. Phys.* **48,** 423.
WINSER K. J., JONES G. O. L. and WILLIAMS P. J. S. 1986 *J. atmos. terr. Phys.* **48,** 893.
WINSER K. J., LOCKWOOD M. and JONES G. O. L. 1987 *Geophys. Res. Lett.* **14,** 957.
WINSER K. J., LOCKWOOD M., JONES G. O. L. and SUVANTO K. 1989 *J. geophys. Res.* **94,** 1439.